

For reprint orders, please contact: reprints@futuremedicine.com

Attenuation of nontargeted cell-kill using a high-density lipoprotein-mimicking peptide–phospholipid nanoscaffold

Research in the development of nanoscale drug carriers primarily focuses on maximizing drug delivery efficiency to tumor tissues. However, less attention has been given to minimizing drug toxicity to nontargeted cells to enhance therapeutic selectivity. **Aim:** Herein, we report on the use of a newly developed high-density lipoprotein-mimicking peptide–phospholipid nanoscaffold (HPPS) to deliver a lipophilic drug, paclitaxel oleate (PTXOL). **Method & Results:** The formulated PTXOL HPPS (120:1) drastically increased therapeutic selectivity by reducing cytotoxicity of PTXOL to nontargeted cells. Using mice bearing targeted (KB) and nontargeted (HT1080) tumors as models, we demonstrated that tumor volume of nontargeted cells was decreased to 57% by PTXOL treatment but increased to 1220% by PTXOL HPPS treatment. However, upon treatment of paclitaxel, PTXOL and PTXOL HPPS, tumor volumes of targeted groups were reduced to 85, 50 and 63%, respectively. **Conclusion:** These data strongly suggest that HPPS can attenuate toxicity of anticancer drugs to nontargeted cells, resulting in cell-killing efficacy only on targeted cells.

KEYWORDS: biomimetic ■ cytosolic delivery ■ drug delivery ■ lipid nanoparticle ■ paclitaxel ■ peptide ■ tumor targeting

Mi Yang^{1,2,3*}, Juan Chen^{1,2*}, Weiguo Cao^{1,2,4}, Lili Ding¹, Kenneth K Ng^{1,2}, Honglin Jin^{1,2,5}, Zhihong Zhang^{1,2,5} & Gang Zheng^{1,2}

¹Campbell Family Cancer Research Institute and Ontario Cancer Institute, University Health Network, Toronto, Canada

²University of Toronto, Toronto, Canada

³Department of Oncology, Drum Tower Hospital Affiliated to School of Medicine and Clinical Cancer Institute of Nanjing University, Nanjing, China

⁴Department of Chemistry, Shanghai University, Shanghai, China

⁵Britton Chance Center for Biomedical Photonics, Wuhan National Laboratory for Optoelectronics-Huazhong University of Science & Technology, Wuhan, China

*Author for correspondence:

Tel.: +1 416 581 7666

Fax: +1 416 581 7667

gang.zheng@uhnres.utoronto.ca

*Authors contributed equally

Nanotechnology has shifted the paradigm of anticancer drug delivery. Small-molecule drugs packed in nanoparticles can improve their solubility, protect them from premature degradation, prolong blood circulation and enhance tumor accumulation through the enhanced permeability and retention effect [1–3]. Moreover, with various tumor-targeting molecules (antibodies, peptides and nucleic acids), nanoparticles can achieve active tumor targeting [4–7]. Numerous studies have demonstrated that by using specific targeting ligands or by tumor-specific biomarker activation, the drug delivery efficiency to targeted tumor tissues is significantly increased, resulting in an improved therapeutic index, hence better therapeutic efficacy [1,8]. However, such an effect is often the direct result of the relative increase of the drug uptake in tumor versus normal tissue ratio and rarely leads to the absolute decrease of drug distribution in normal tissues. Therefore, these agents will still encounter side effects such as bone marrow suppression, gastric erosion, renal toxicity, cardiomyopathy and neurotoxicity [9]. Attenuation of drug toxicity to nontargeted tissues (protecting normal tissues from collateral damage) is another important direction to improve therapeutic index and drug efficacy. Selective protection of nontargeted cells requires nanoparticle carriers to shield the encapsulated toxic payloads from nonspecific uptake or premature release until they reach targeted cells. Selective protection of normal cells will reduce systemic side effects and increase clinical

tolerable dose, which will ultimately improve the impact of chemotherapy. The goal of this study was to explore the utility of a new nanoparticle carrier in protecting nontargeted cells while asserting toxicity against targeted cells.

We recently introduced a high-density lipoprotein (HDL)-mimicking peptide–phospholipid nanoscaffold (HPPS) as a powerful vehicle for direct cytosolic payload delivery, thus bypassing the formidable threat posed by the endosomal trapping of drug carriers [10]. HPPS is composed of the phospholipid, cholesteryl oleate and an amphipathic α -helical peptide, apolipoprotein A-1 (ApoA-1) mimetic, which are all highly biocompatible [11–13]. The interaction between the self-assembled peptide network and the colloidal phospholipid monolayer enables HPPS to mimic the behavior of plasma-derived HDL in both its structural and functional properties (e.g., size, lipophilic payload, scavenger receptor class B type 1 [SRB1] specificity and pharmacokinetics) [10]. Like spherical HDL, HPPS is highly monodisperse with a distinct sub-30-nm core-shell structure; thus, it is able to diffuse freely through interstitial spaces (<40 nm) [14], a key advantage for the enhancement of both accumulation and internalization in solid tumors [10]. HPPS also mimics the plasma HDL in its long circulation half-life and its ability to target the SRB1 [10], which is overexpressed on a number of tumor cells [15–17]. The SRB1 pathway is particularly attractive for anticancer drug delivery because it mediates the selective transport of

future
medicine part of fsg

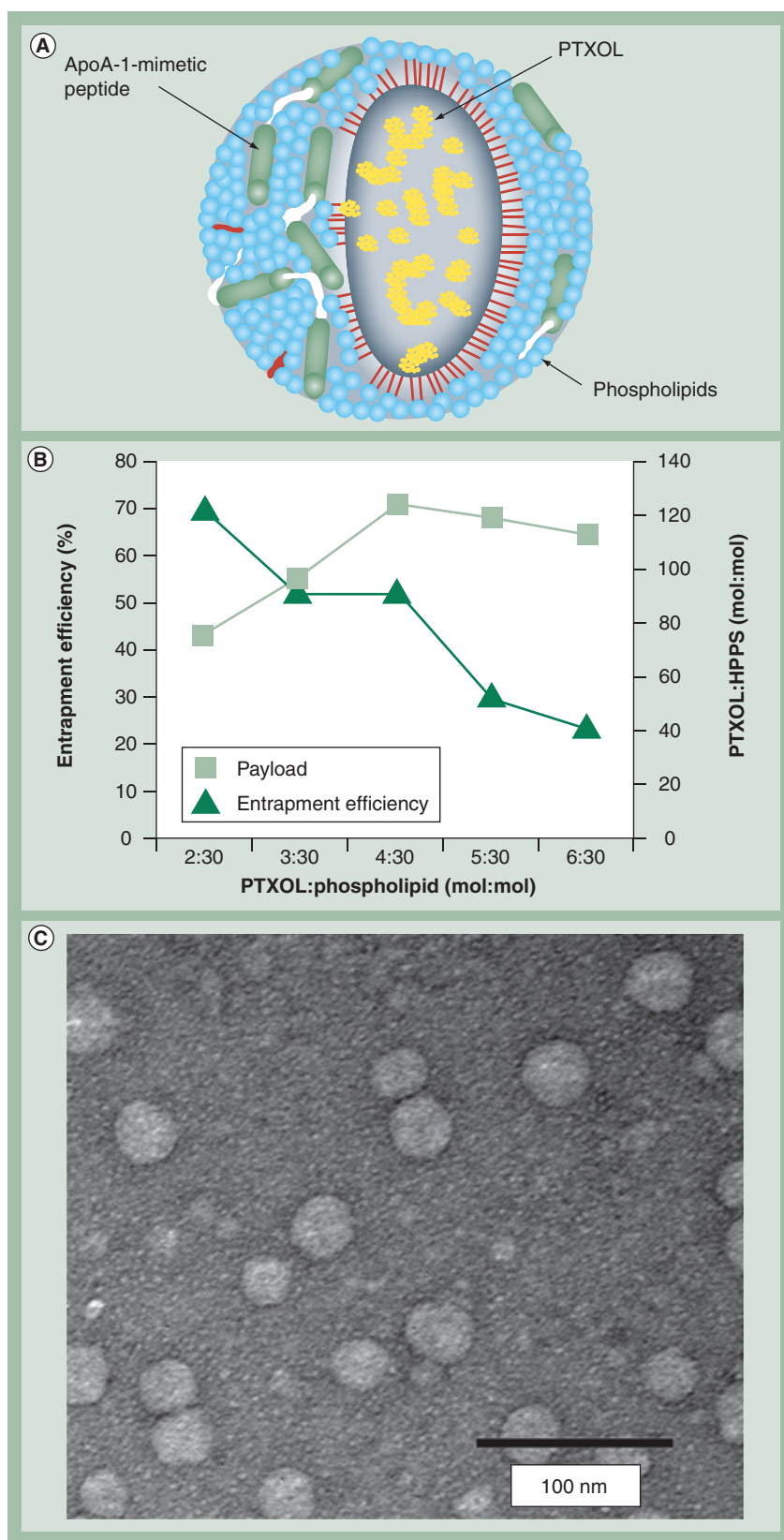


Figure 1. Paclitaxel oleate. (A) Schematic figure of PTXOL HPPS. (B) Optimization of PTXOL HPPS formulation by adjusting the ratio of PTX and phospholipids. (C) Transmission electron microscope image of PTXOL HPPS. ApoA-1: Apolipoprotein A-1; HPPS: High-density lipoprotein-mimicking peptide-phospholipid nanoscaffold; PTX: Paclitaxel; PTXOL: Paclitaxel oleate.

cholesterol esters from HDL directly into the cytosol of targeted cells [18,19]. We have shown that HPPS is capable of exploiting this unique nonendocytic uptake mechanism for the direct cytosolic payload delivery [10]. In addition, HPPS exhibits effective shielding properties that could protect the payload before it enters the targeted cells [10]. Finally, HPPS is a modular platform with the capability to carry a range of diagnostic and therapeutic payload molecules and versatile tumor-targeting ligands. Together, these features resulted in a **simple and robust nanocarrier** for efficient tumor-targeted drug delivery. We hypothesized that using HPPS for anticancer drug delivery could enhance targeting therapy, not only by an effective therapeutic effect to targeted cells, but also by attenuating toxicity to normal tissues. To test this hypothesis, our study design features the following drug selection and *in vitro* and *in vivo* models.

Drug selection

A lipophilic prodrug of paclitaxel (PTX), PTX oleate (PTXOL) [20,21], is used as a prototype drug to be loaded into HPPS as depicted in **FIGURE 1A**. This prodrug releases PTX with facile enzymatic hydrolysis of the fatty acid esters and causes cell death by disrupting the normal microtubule dynamics required for cell division [21]. The lipid anchor of PTXOL is expected to enable its stable incorporation into the hydrophobic core of HPPS.

In vitro & *in vivo* models

A human KB cell line (KB), which expresses a high level of SRB1 (SRB1⁺), was selected as the targeted cell to investigate the therapeutic effect of the PTXOL-loaded HPPS, denoted as PTXOL HPPS. A human fibrosarcoma cell line (HT1080), which has a low level of SRB1 (SRB1⁻) expression was chosen as the nontargeted cell to investigate the protective function of PTXOL HPPS. Chemotherapeutic drugs often damage cells by interfering with DNA replication or cellular metabolism. Thus, tumor cells, which proliferate much faster than normal cells, are more sensitive to drug damage [22]. Therefore, if HPPS can attenuate the toxicity of PTXOL to nontargeted tumor cells, it will provide strong evidence for its protective function for nontargeted normal cells.

Materials & methods

Materials

1,2-dimyristoyl-sn-glycero-3-phosphocholine (DMPC) was obtained from Avanti Polar Lipids Inc. (AL, USA). Cholesteryl oleate (CO) and oleoyl chloride were obtained from Sigma-Aldrich

Co. (MO, USA). PTX was obtained from LC laboratories (MA, USA). The cell culture media RPMI 1640 medium, fetal bovine serum, 3-(4,5-dimethylthiazole-2-yl)-2,5-diphenyltetrazoliumbromide (MTT) and trypsin-ethylenediaminetetraacetic acid (EDTA) solution were all purchased from Gibco-Invitrogen Co. (CA, USA). The ApoA-1 mimetic peptide (AP), Ac-FAEKFKAEVKDYFAKFW, was synthesized on a PS-3 peptide synthesizer (Protein Technologies). 1,1'-dioctadecyl-3,3,3',3'-tetramethylindotricarbocyanine iodide bisoleate (DiRBOA, a lipid-anchored near-infrared fluorescent dye) and PTXOL were synthesized by the previously reported methods [21,23]. KB (SRB1⁺) and HT1080 (SRB1⁻) cell lines were purchased from the American Type Culture Collection.

■ Nanoparticles preparation

High-density lipoprotein-mimicking peptide–phospholipid nanoscaffold and DiRBOA-loaded HPPS (DiRBOA HPPS) was prepared using previously described methods [10]. PTXOL-loaded HPPS (PTXOL HPPS) was prepared by combining 3 μmol DMPC, 0.1 μmol CO and 0.4 μmol PTXOL in 200 μl of chloroform and mixed for 5 min. The mixture was then dried under a stream of nitrogen gas to form a thin lipid film and further dried under vacuum for 1 h. A total of 1 ml of phosphate-buffered saline (PBS, pH 7.5) was added to the dried lipid film, followed by vortexing for 5 min and sonication under 48°C for 1 h. The turbid emulsion became transparent after adding 2 mg of AP (dissolved in 1 ml PBS) and was stored at 4°C overnight. The mixture was then purified by size exclusion chromatography (HiLoad 16/60 Superdex 200 pg, GE Healthcare) with Tris buffered saline (10 mM Tris–HCl, 0.15 M NaCl, 1 mM EDTA, pH 7.5) at a flow rate of 1 ml·min⁻¹. Fractions at the retention time from 55 to 65 min were collected and concentrated using a centrifugal filter device (10,000 MW, Amicon, Millipore). The resulting PTXOL HPPS was stored under 4°C until use (SUPPLEMENTARY FIGURE 1A, see online www.futuremedicine.com/doi/suppl/10.2217/nmm.11.10).

■ Characterization of PTXOL HPPS

Determination of nanoparticle compositions

The molar concentrations of DMPC, CO and AP were determined using a previously reported method [10]. A reverse-phase high-performance liquid chromatography protocol was developed to quantify the molar concentration of PTXOL

in HPPS. First, the retention time of PTXOL was determined by a HPLC mass spectrometry system (Waters 2695 controller with a 2996 photodiode array detector and a Waters ZQ™ mass detector, USA) using the following method: solvent A = 0.1% trifluoroacetic acid in water, solvent B = acetonitrile; gradient: from 60% A + 40% B to 50% A + 50% B for 5 min, then to 20% A + 80% B for 30 min and further to 100% B for 5 min; flow rate: 0.5 ml·min⁻¹. Samples were run on a Waters XBridge™-C3 column (2.5 μm, 4.6 × 150 mm) and absorbance was read at 229 nm. PTXOL had a column retention time of approximately 35.8 min identified by the corresponding ESI-Mass (cal. 1118.4, found 1118.7, SUPPLEMENTARY FIGURE 1B). The area under the peak was calculated using numerical integration (Simpson's rule). A standard curve was then made using known amounts of PTXOL in dimethylformamide. To determine the PTXOL payload in the formulation, PTXOL was extracted from the nanoparticle by using organic solvent extraction. Briefly, 100 μl of PTXOL HPPS was extracted with 300 μl of chloroform, vortexed for 3 min, and then centrifuged at 12,000 rpm for 10 min. The organic phase was collected, dried, redissolved in dimethylformamide and injected into the HPLC mass spectrometry for quantification of the PTXOL concentration (C_{PTXOL}). The payload of PTXOL per HPPS was determined with EQUATION 1:

$$\text{Payload (mol/mol)} = C_{\text{PTXOL}} \times N / C_{\text{DMPC}}$$

(C_{DMPC} : molar concentration of DMPC; N: number of DMPC molecules per HPPS particle)

Morphology & size measurement

Transmission electron microscopy was performed on a modern Hitachi H-7000 transmission electron microscope (Hitachi, Inc., Japan) equipped with a digital image acquisition system to determine the morphology and size dispersion of PTXOL HPPS stained with 2% uranyl acetate. The particle size distributions of PTXOL HPPS was measured by dynamic light scattering photon correlation spectroscopy (Zetasizer Nano-ZS90; Malvern Instruments, UK) utilizing a 4.0 mW He–Ne laser operating at 633 nm and a detector angle of 90°.

■ Flow cytometry study

Human KB and HT1080 cells were incubated in RPMI 1640 supplemented with 10% fetal bovine serum at 37°C in a humidified atmosphere with 5% CO₂. Cells were seeded in six-well plates at a density of 2 × 10⁵ cells per well and incubated for 24 h at 37°C in an atmosphere of 5% CO₂ in a humidified incubator. The

medium was removed and the cells were rinsed with PBS. The cells were then incubated with 10 μM of DiRBOA HPPS for 5 min, 10 min, 20 min, 30 min, 1 h, 3 h, 6 h, 12 h and 16 h, respectively. After removal of DiRBOA HPPS, cells were incubated further in culture medium to 24 h then transferred to a 15 ml centrifuge tube with 2 ml of PBS. Subsequently, cells were centrifuged at 1300 rpm for 6 min and the PBS was removed. This rinsing procedure was repeated three times. The cells were then fixed by 2% paraformaldehyde solution for 10 min. After fixing, the cells were centrifuged and rinsed with PBS twice. The fluorescence intensities of the cells were measured by a Cytomics FC 500 series flow cytometry system from Beckman Coulter (excitation: 633 nm; emission: 660–690 nm). Autofluorescence from the untreated cells was minimal. The maximum cell number count was 10,000 for all samples.

■ *In vitro* toxicity study

In vitro toxicity of PTXOL HPPS was determined on KB and HT1080 cells and quantified by standard MTT assays [24]. Cells were seeded in a 96-well plate at a density of 8000 cells per well. Once cells reached 80% confluence, the medium was replaced with 200 μl culture medium containing PTX (8 μM), PTXOL (8 μM), PTXOL HPPS (containing PTXOL 8 μM and HPPS 0.07 μM), PTXOL HPPS with 20-fold molar excess of HDL (containing PTXOL 8 μM , HPPS 0.07 μM and HDL 1.4 μM), and HPPS (0.07 μM). One row of the 96-well plates was used as a control with 200 μl culture medium only. After 6 h incubation, the drug solutions were removed and the cells were washed twice with PBS and allowed to grow for an additional 42 h. The MTT compound was then added to the medium at 0.5 $\text{mg}\cdot\text{ml}^{-1}$. After 2 h the medium was removed and replaced with 150 μl of 1:1 DMSO/70% isopropanol in 0.1 M HCl. The absorbance at 570 nm was measured on a Bio-Tek ELx model 800 (MTX Lab System, VA, USA).

■ Mouse xenografts & *in vivo* anti-tumor study

All animal studies were following protocols approved by the Animal Care Committee at the University Health Network. Nude mice (female, 6–7 weeks old) were inoculated with 2×10^6 KB cells or HT1080 cells (in 100 μl PBS) subcutaneously in the right flanks. Tumor dimensions were measured with vernier calipers and volumes were calculated as follows: tumor

volume (mm^3) = width² (mm^2) \times length (mm)/2. When tumors reached 100–300 mm^3 in size (7–12 days after tumor cell implantation), the animals were randomized into the following treatment groups: PTX (23 $\mu\text{mol}\cdot\text{kg}^{-1}$, dissolved in 0.3 ml of saline containing 10% Cremophor EL and 10% ethanol), PTXOL (23 $\mu\text{mol}\cdot\text{kg}^{-1}$, dissolved in 0.3 ml saline containing 10% Cremophor EL and 10% ethanol), PTXOL HPPS (containing PTXOL 23 $\mu\text{mol}\cdot\text{kg}^{-1}$, HPPS 0.2 $\mu\text{mol}\cdot\text{kg}^{-1}$, dissolved in 0.3 ml saline), HPPS (0.2 $\mu\text{mol}\cdot\text{kg}^{-1}$, dissolved in 0.3 ml saline) and saline (0.3 ml). Each treatment group received tail vein injections once a week for 3 weeks. Tumor volumes were measured twice a week. The last dose was provided after 1 week (21 days after the first dose given), mice were sacrificed and tumors were excised and collected to check size and weight. Percentage change in tumor volume was calculated using EQUATION 2:

$$\text{Tumor volume change} = (\text{volume}_{\text{current}} - \text{volume}_{\text{initial}}) / \text{volume}_{\text{initial}} \times 100\%$$

(volume_{current}: current tumor volume, volume_{initial}: initial tumor volume before treatment)

■ *In vivo* toxicity study of HPPS

To assess the tolerability of HPPS, 2000 $\text{mg}\cdot\text{kg}^{-1}$ HPPS (based on phospholipid concentration) was given to five nude mice (female, 6–7 weeks old) through the tail vein and 0.5 ml saline were given to the other five mice as controls. After injection, mice were monitored for health and the body weights were measured every 3 days. At 1, 8 and 15 days postinjection, blood samples (200 μl each) were collected from the saphenous vein to test peripheral blood cells and liver function. At 21 days postinjection, mice were sacrificed and their organs (heart, liver, spleen, kidney and lung) were excised, fixed in 10% formalin, embedded in paraffin, sectioned and stained with hematoxylin and eosin for histological analysis.

■ Statistical analysis

The Student's *t*-test (two tailed) was used to determine significant differences between *in vitro* and *in vivo* anti-tumor efficacy in experiments. *P*-values less than 0.05 were considered significant.

Results

■ Synthesis & characterization of PTXOL HPPS nanoparticles

Paclitaxel oleate, a lipophilic derivative of PTX, was used as a prototype drug to evaluate the drug delivery capacity of HPPS. The PTXOL

HPPS formulation was prepared and optimized by changing the ratio of PTXOL to phospholipids. As shown in FIGURE 1B, the increase of PTXOL to lipid ratio led to the increase of PTXOL payload, which reached maximum when the ratio exceeded 4:30. Meanwhile, the PTXOL entrapment efficiency continuously decreased with an increase in the PTXOL to lipid ratio. Thus, the 4:30 PTXOL to lipid ratio was selected for the preparation of PTXOL HPPS for all subsequent studies because of its relatively high payload and good entrapment efficiency. The resultant PTXOL HPPS formulation contained 120 PTXOL per particle (mol/mol) and its PTXOL recovery was determined to be 51.9% from the starting material. The transmission emission microscopy data (FIGURE 1C) showed that the PTXOL HPPS formed a monodispersed spherical particle with a diameter of 21.8 ± 3.4 nm (dynamic light scattering data, SUPPLEMENTARY FIGURE 1C). HPPS and fluorescent DiRBOA HPPS were also prepared as controls, according to the previously reported protocol [10], to reaffirm its intracellular delivery mechanism and to provide guidance for setting the treatment protocols through its fluorescent properties.

■ Differential kinetics of HPPS payload delivery in target versus nontargeted cells

We have previously demonstrated that HPPS can deliver payload specifically to SRB1⁺ cells by confocal imaging using fluorescently labelled DiRBOA HPPS [10]. To further understand this interaction, we studied the kinetics of HPPS payload delivery using flow cytometry in KB (SRB1⁺) cells versus HT1080 (SRB1⁻) cells with a surrogate fluorescent payload (DiRBOA). All cell-associated fluorescence was normalized to the saturated fluorescence signal of DiRBOA HPPS in KB cells. The results indicated that the fluorescence associated with KB cells upon DiRBOA HPPS treatment was rapid, reaching 60 and 93% of maximum cell-associated fluorescence after 30 min and 6 h, respectively (FIGURE 2). In comparison, there was limited association observed by HT1080 cells and this process proceeded over an extended period of time. This association was found to be less than 7% at the 30 min time point and did not become saturated after 16 h of incubation. Based on the above flow cytometry results, we found 6 h to be the shortest incubation time to observe maximal binding to KB cells and equated to a 5.4-fold greater association when compared with HT1080 cells.

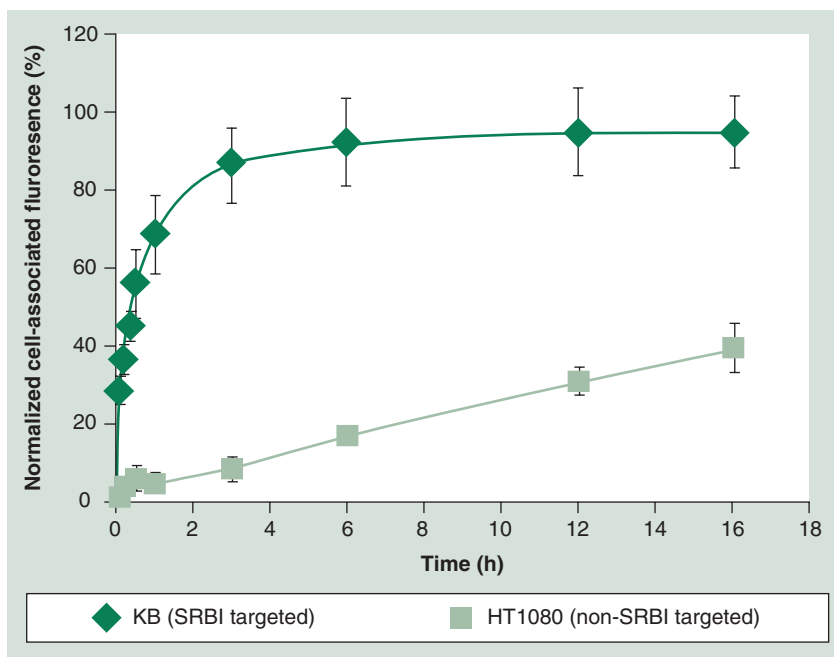


Figure 2. Fluorescent dye core-loaded HPPS (DiRBOA HPPS) was used to elucidate the differential kinetics of HPPS on scavenger receptor class B type 1 targeted (KB) cells and nontargeted (HT1080) cells. Mean values \pm SD, $n = 3$. All data were normalized to the saturated uptake of DiRBOA HPPS in KB cells. DiRBOA: 1,1'-dioctadecyl-3,3,3',3'-tetramethylindotricarbocyanine iodide bisoleate; HPPS: High-density lipoprotein-mimicking peptide–phospholipid nanoscaffold; SD: Standard deviation; SRB1: Scavenger receptor class B type 1.

For these reasons, we utilized 6 h as the optimal incubation time for subsequent PTXOL HPPS efficacy studies.

■ Selective *in vitro* cytotoxicity of PTXOL HPPS to targeted versus nontargeted cells

After validating the differential kinetics of HPPS payload delivery and determining the optimal drug incubation time point, we next studied the selective cytotoxicity of PTXOL HPPS on KB (SRB1⁺) and HT1080 (SRB1⁻) cells, where PTX, PTXOL and HPPS were used as controls. As shown in FIGURE 3, HPPS alone (vehicle control) did not show any toxicity to cells in the experiment. The drug controls, PTX and PTXOL induced very similar cell toxicity to either KB or HT1080 cells, suggesting that the PTXOL prodrug can generate similar anti-tumor efficacy as PTX. Compared with KB cells, HT1080 cells were found to be more sensitive to PTX and PTXOL treatments. Upon PTX treatment, cell viabilities of KB and HT1080 cells were 45 and 12%, respectively. Upon PTXOL treatment, cell viabilities in KB and HT1080 cells were 42 and 6%, respectively. Loading PTXOL into HPPS significantly decreased the cytotoxicity of PTXOL HPPS to nontargeted HT1080

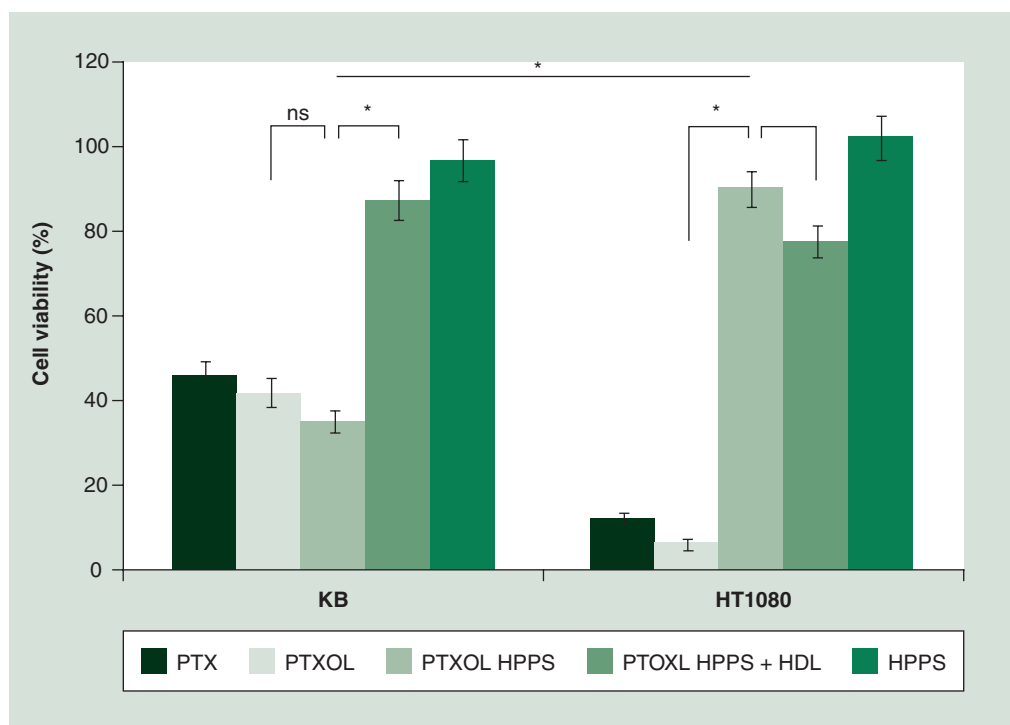


Figure 3. Evaluation of the *in vitro* therapeutic response of paclitaxel oleate high-density lipoprotein-mimicking peptide-phospholipid nanoscaffold to SRB1 targeted KB cells and nontargeted HT1080 cells using the MTT assay. Mean values \pm SD, $n = 5$.

* $p < 0.01$, ns, $p > 0.05$. Nonpaired two-tailed Student's t-test.

HDL: High-density lipoprotein; HPPS: High-density lipoprotein-mimicking peptide-phospholipid nanoscaffold; MTT: 3-(4,5-dimethylthiazole-2-yl)-2,5-diphenyltetrasodiumbromide;

ns: Not significant; PTX: Paclitaxel; PTXOL: Paclitaxel oleate; SRB1: Scavenger receptor class B type 1.

cells ($p < 0.01$) (the cell viability was 6% for PTXOL treatment and 91% for PTXOL HPPS treatment). This is a clear indication that HPPS is able to shield PTXOL from nontargeted cells (HT1080). Nevertheless, PTXOL HPPS maintained its therapeutic effect against targeted cells (35%) since it induced similar toxicity in KB cells as the free PTX (45%) or PTXOL (42%) did. Moreover, this therapeutic effect was blocked by a 20-fold excess of native HDL. The aforementioned data strongly suggests that HPPS can effectively deliver drug to cells through the SRB1-mediated pathway and can effectively attenuate toxicity of anticancer drugs to nontargeted cells, but retain its cytotoxicity against targeted cells.

■ Selective *in vivo* anti-tumor efficacy of PTXOL HPPS to targeted versus nontargeted cells

The *in vivo* anti-tumor efficacy study was performed on mice bearing either KB or HT1080 tumors. PTXOL HPPS was given once a week for 3 weeks by intravenous injection. Saline, PTX, PTXOL and HPPS were also given as controls. The size of all tumors were tracked by monitoring

tumor dimension twice a week and compared with their initial size. As shown by the tumor growth curve in **FIGURE 4A**, the tumor size continually increased following administration with HPPS and saline, while PTX and PTXOL effectively inhibited tumor growth. The final KB and HT1080 tumor volumes, at 21 days after the first dose were reduced to 85.6 ± 5.6 and $31.3 \pm 1.5\%$, respectively for PTX treatment and 50.2 ± 21.7 and $57.4 \pm 30.3\%$, respectively for PTXOL treatment. This showed both PTXOL and PTX inhibited the tumor growth of targeted and nontargeted cells. However, after loading PTXOL into HPPS, PTXOL HPPS was only able to suppress the tumor growth of the targeted cells, but not the nontargeted cells. The final KB tumor volume decreased to 63.4 ± 15.0 , while HT1080 tumor volume increased to $1220.5 \pm 531.1\%$. This was also evident in excised tumor images (**FIGURE 4B**) showing the significant difference between *in vivo* therapeutic efficacy of PTXOL HPPS to targeted and nontargeted cells. Since some normal tissues, such as liver, also express a high level of SRB1, we tested liver function of the mice administrated with PTXOL HPPS to investigate the side effects of PTXOL HPPS on

normal tissues. When compared with the saline control mice, no significant liver function damage was detected under our *in vivo* experimental conditions (SUPPLEMENTARY TABLE 1). Collectively, these *in vivo* data are consistent with the *in vitro* findings and provided convincing evidence that HPPS is not only able to effectively deliver anticancer drugs to targeted cells, but is also capable of attenuating the damage to nontargeted cells, resulting in an improved therapeutic index.

■ Validation of HPPS's biocompatibility

To further support the potential clinical utility of HPPS for anticancer drug delivery, we evaluated its acute toxicity by intravenously administering nude mice with 2000 mg·kg⁻¹ of HPPS (the highest single test dose limited according to US FDA guidelines) and assessing its behavioral,

biochemical and physical effects. Mice injected with 0.5 ml of saline served as controls. The HPPS treated groups did not show any abnormality in behavior. When compared with saline controls, the HPPS treated group did not show any measurable adverse effect on blood cells or liver function at 1, 8 and 15 days postinjection (FIGURE 5). The peripheral blood cells including white blood cells, red blood cells and platelets were all within the normal range. Analysis of liver enzymes such as alanine aminotransferase and alkaline phosphatase did not show potential toxicity. Furthermore, within 21 days, the body weight of the HPPS-treated group did not decrease and was not significantly different to that of the control group ($p>0.5$) (FIGURE 6A). Finally, morphological and pathological examinations of the organs (FIGURE 6B) revealed that there was no

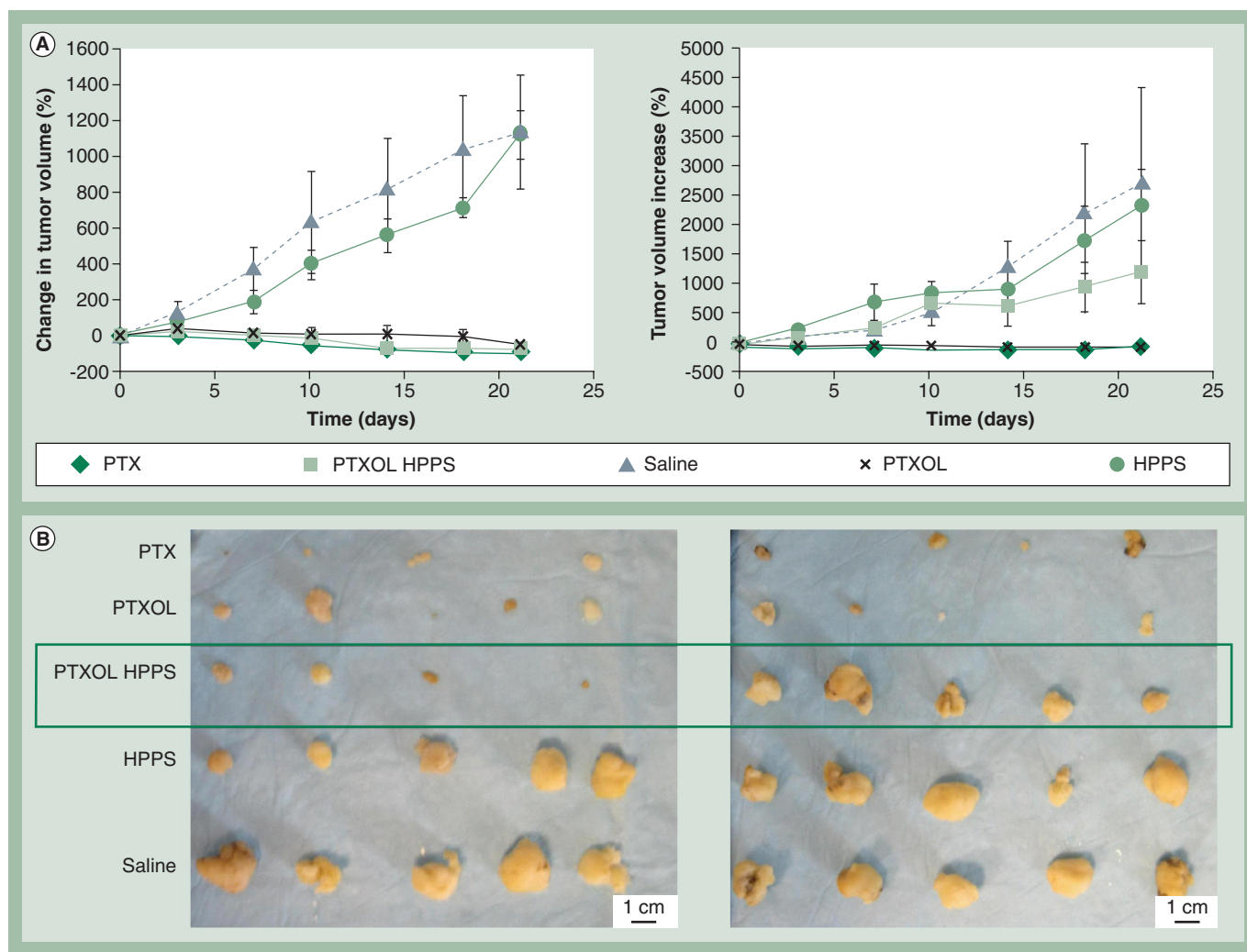


Figure 4. Evaluation of *in vivo* anti-tumor efficacy on nude mice bearing SRB1 targeted KB tumor and nontargeted HT1080 tumor. (A) Real-time monitoring the tumor volume change (mean values \pm SD, $n = 5$). (B) *Ex vivo* photography of tumors excised from mice after 21 days treated with PTX, PTXOL HPPS and saline.

HPPS: High-density lipoprotein-mimicking peptide–phospholipid nanoscaffold; PTX: Paclitaxel; PTXOL: Paclitaxel oleate; SD: Standard deviation; SRB1: Scavenger receptor class B type 1.

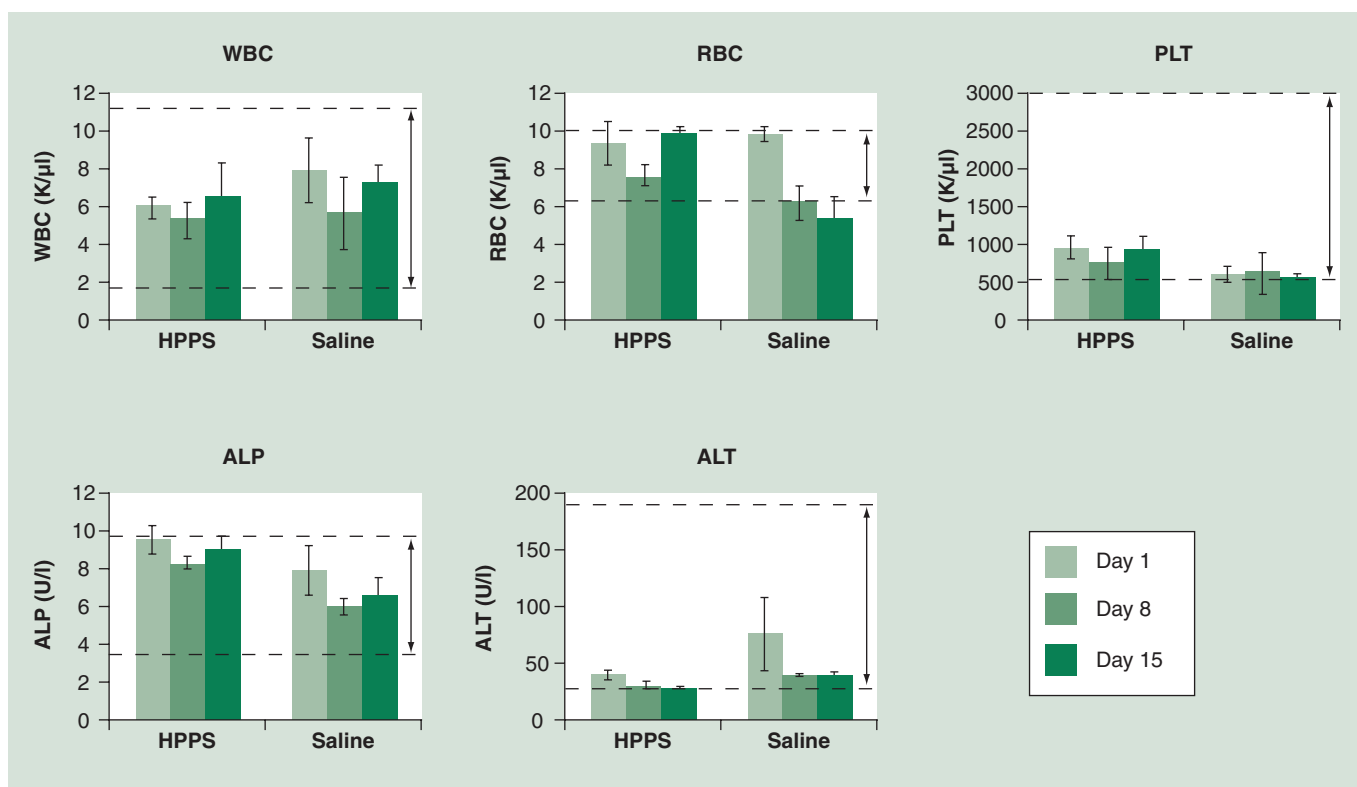


Figure 5. Acute toxicity studies of high-density lipoprotein-mimicking peptide–phospholipid nanoscaffold. Mice ($n = 5$) were injected with $2000 \text{ mg}\cdot\text{kg}^{-1}$ HPPS intravenously. Control group ($n = 5$) were injected with saline. No adverse effect was observed on blood cells and liver functions. Normal range is between the two dashed lines.

ALP: Alkaline phosphatase; ALT: Alanine transaminase; HPPS: High-density lipoprotein-mimicking peptide–phospholipid nanoscaffold; PLT: Platelet; RBC: Red blood cell; WBC: White blood cell.

potential toxicity or damage to the heart, liver, kidney, spleen and lung as no necrosis, inflammatory reactions, fibrosis or local fatty degeneration were observed in the tissues after 21 days treatment. These data provide strong evidence that HPPS is a safe vehicle for drug delivery.

Discussion

Developing nanoparticle carriers to transport a large bolus of drug molecules into cytosolic compartments of cancer cells has become a highly active research area in nanomedicine [25]. This is because the sites of action for most cancer drugs are often cytosolic organelles and the cytosolic delivery might offer a means to evade efflux transporters such as multidrug resistance proteins and P-glycoproteins [26]. However, the challenges are abundant, for example:

- Nanoparticle carriers are required to carry a large payload of drug that must be protected from extracellular degradation.
- Nanoparticle internalization may lead to drug entrapment in closed vesicles (endosomes or phagosomes), resulting in decreased drug efficacy.

High-density lipoprotein is an endogenous nanocarrier possessing many attractive features for drug delivery (e.g., ultra small size, favorable surface properties and selective delivery of cholesterol esters to the cytosol of cells by the SRB1 mediated pathway). Using HDL for anticancer drug delivery has been reported by McConathy *et al.* [27,28]. One potential hurdle in developing HDL as a clinically viable nanocarrier lies in the fact that lipoproteins are isolated from fresh donor plasma, which might result in batch-to-batch variation and pose some scale-up challenges. By mimicking HDL, the HPPS nanocarrier offers a new avenue for the delivery of intracellular active anticancer drugs because of its ability to directly transport a functional payload to the cytosol of cancer cells without going through endolysosomal trafficking, and its increased capability in its flexibility and scalability.

Here, we examined the capability of HPPS for anticancer drug delivery using PTXOL HPPS as a model. The hydrophobic core of HPPS carries a high payload of PTXOL (120 PTXOL/per particle) while maintaining its size and monodispersity (FIGURE 1C). PTXOL HPPS is stable in both

storage conditions (4°C) (SUPPLEMENTARY FIGURE 2A) and in serum at 37°C (SUPPLEMENTARY FIGURE 2B). Like liposomes and other lipid nanoparticles, HPPS is also highly biocompatible. Evidence of the biocompatibility of the HPPS was obtained from an *in vivo* acute toxicity test. At the very high intravenous dose of 2000 mg·kg⁻¹, the HPPS-treated groups showed no abnormality in behavior, no measurable adverse effect on blood cells and liver function, no decrease in body weight, and no toxicity or damage to main organs, providing strong evidence that HPPS is a safe nanocarrier for lipophilic drug delivery.

For functional studies of PTXOL HPPS on targeted cells (SRB1⁺), the efficient therapeutic response was achieved presumably due to both the SRB1-mediated cytosolic payload delivery and the long circulation half-life of HPPS [10]. By using a surrogate fluorescent payload, the SRB1-specificity of HPPS was reaffirmed. Furthermore, flow cytometry data revealed a significant contrast in the speed of HPPS payload delivery between targeted versus nontargeted cells. The majority of HPPS payload (60% maximum cell-associated fluorescence) was delivered to targeted cells within

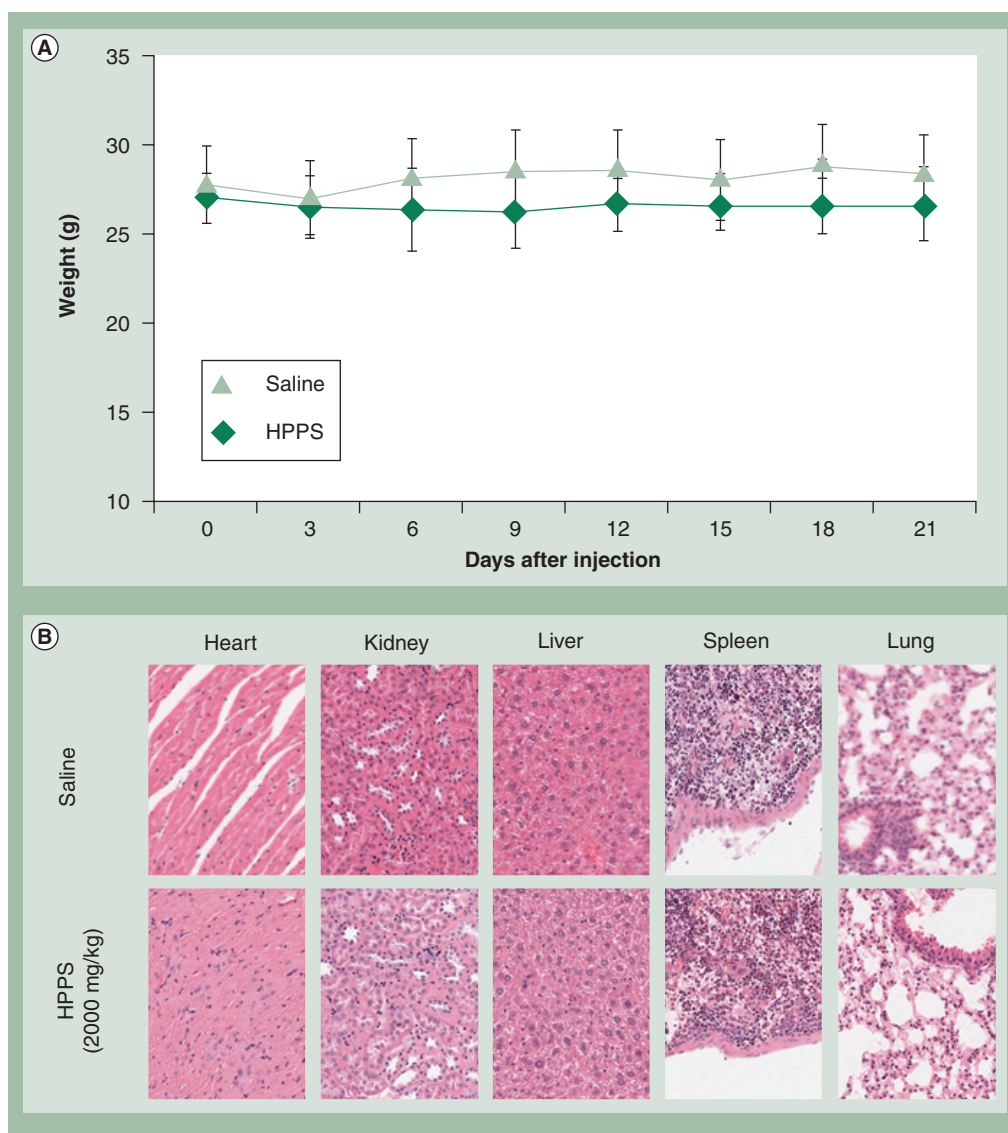


Figure 6. Body weight and toxicity studies of high-density lipoprotein-mimicking peptide–phospholipid nanoscaffold. (A) Real-time monitoring of mice body weight after injected with 2000 mg·kg⁻¹ high-density lipoprotein-mimicking peptide–phospholipid nanoscaffold and saline. (B) The morphological and pathological examinations of the organs after 21 days treated with 2000 mg·kg⁻¹ HPPS and saline. The results revealed that there was no potential toxicity or damage to the heart, liver, kidney, spleen and lung. HPPS: High-density lipoprotein-mimicking peptide–phospholipid nanoscaffold.

30 min, whereas only 7% of HPPS payload was associated with nontargeted cells within the same timeframe (FIGURE 2). Compared with the distribution half-life (0.34 h) and the elimination half-life (5.8 h) of Taxol® (the Cremophor EL formulation of PTX) [29], using HPPS to deliver PTXOL can prolong drug blood circulation, with a payload distribution half-life of 2.6 h and an elimination half-life of 17.6 h (SUPPLEMENTARY FIGURE 3), thus providing more time for the PTXOL HPPS to reach its target site to improve the targeting delivery efficiency. Therefore, HPPS can be used to effectively deliver anticancer drugs to targeted cancer cells.

A key finding of this study is the marked attenuation of *in vivo* cytotoxicity of PTXOL HPPS against nontargeted cells with the SRB1⁻ tumor (HT1080) used as a model. The highly protective function of PTXOL HPPS to nontargeted cells is likely due to the drug-shielding ability of HPPS. It was evident that PTXOL HPPS significantly reduced the cytotoxicity of PTXOL to HT1080 cells (SRB1⁻), which was more sensitive to PTXOL treatment than KB cells (SRB1⁺) (FIGURE 3).

The attractive properties of HPPS make it a powerful nanoparticle platform for anticancer drug delivery. In our previous studies, EGF-conjugated HPPS showed a coordinated dual receptor (EGF receptor and SRB1) targeting phenomenon leading to enhanced payload delivery [30]. Furthermore, HPPS has been successfully loaded with either fluorescent dye or photodynamic therapy agents [16]. The combined diagnostic and therapeutic use of targeted HPPS nanoparticle platforms enables image-guided drug delivery, thus providing new potentials for clinical cancer diagnosis and treatment.

Conclusion

In summary, HPPS selectively delivered high payload of PTXOL to tumor cells through a direct cytosolic transport mechanism, inducing effective therapeutic activity only to targeted cells while attenuating cytotoxicity of anticancer

drugs to nontargeted cells. The selective protection provides a promising strategy to reduce therapeutic side effects and increase clinical tolerable doses, which could ultimately lead to the improved impact of chemotherapy.

Future perspective

The direct cytosolic delivery and the drug-shielding ability of HPPS make it a powerful nanoparticle platform for anticancer drug delivery. Besides targeting to its natural SRB1 receptor, HPPS could be redirected to other tumor specific biomarkers (e.g., EGF receptor). Furthermore, HPPS is capable of carrying a wide range of imaging and therapeutic agents including fluorescent probes, photodynamic therapy agents and siRNAs. The combined diagnostic and therapeutic use of targeted HPPS could enable image-guided drug delivery, providing new potentials for clinical cancer diagnosis and treatment.

Financial & competing interests disclosure

This study was conducted with the support of the Canadian Institutes of Health Research, the Ontario Institute for Cancer Research through funding provided by the Government of Ontario, the China-Canada Joint Health Research Initiative (CIHR CCI-102936 & NSFC-3091120489), the Natural Sciences and Engineering Research Council of Canada, the Ontario ministry of Health and Long Term Care, and the Joey and Toby Tanenbaum/Brazilian Ball Chair in Prostate Cancer Research. The authors have no other relevant affiliations or financial involvement with any organization or entity with a financial interest in or financial conflict with the subject matter or materials discussed in the manuscript apart from those disclosed.

No writing assistance was utilized in the production of this manuscript.

Ethical conduct of research

The authors state that they have obtained appropriate institutional review board approval or have followed the principles outlined in the Declaration of Helsinki for all human or animal experimental investigations. In addition, for investigations involving human subjects, informed consent has been obtained from the participants involved.

Executive summary

- High-density lipoprotein-mimicking peptide-phospholipid nanoscaffold (HPPS) can encapsulate a high payload of lipophilic drugs (e.g., paclitaxel oleate) in its hydrophobic core to form a monodispersed spherical particle (120 paclitaxel oleate per particle) with a diameter of 22 nm.
- HPPS can selectively deliver its payload to tumor cells through a direct cytosolic transport mechanism.
- HPPS is not only able to deliver anticancer drugs to targeted cells effectively, but is also capable of attenuating their damage to nontargeted cells.
- The selective protection to nontargeted cells provides a promising strategy to reduce therapeutic side effects and increase clinical tolerable dose, which could ultimately lead to the improved impact of chemotherapy.

Bibliography

Papers of special note have been highlighted as:
 ■ of interest

- 1 Davis ME, Chen ZG, Shin DM: Nanoparticle therapeutics: an emerging treatment modality for cancer. *Nat. Rev. Drug Discov.* 7(9), 771–782 (2008).
- 2 Maeda H: Tumor-selective delivery of macromolecular drugs via the EPR effect: background and future prospects. *Bioconjug. Chem.* 21(5), 797–802 (2010).
- 3 Torchilin VP: Recent advances with liposomes as pharmaceutical carriers. *Nat. Rev. Drug Discov.* 4(2), 145–160 (2005).
- 4 Lu W, Zhang G, Zhang R *et al.*: Tumor site-specific silencing of NF- κ B p65 by targeted hollow gold nanosphere-mediated photothermal transfection. *Cancer Res.* 70(8), 3177–3188 (2010).
- 5 McCarthy JR, Kelly KA, Sun EY, Weissleder R: Targeted delivery of multifunctional magnetic nanoparticles. *Nanomedicine* 2(2), 153–167 (2007).
- 6 Soman NR, Baldwin SL, Hu G *et al.*: Molecularly targeted nanocarriers deliver the cytolytic peptide melittin specifically to tumor cells in mice, reducing tumor growth. *J. Clin. Invest.* 119(9), 2830–2842 (2009).
- 7 Wang H, Chen X: Applications for site-directed molecular imaging agents coupled with drug delivery potential. *Expert Opin. Drug Deliv.* 6(7), 745–768 (2009).
- 8 Sawyers C: Targeted cancer therapy. *Nature* 432(7015), 294–297 (2004).
- 9 Zhang L, Gu FX, Chan JM, Wang AZ, Langer RS, Farokhzad OC: Nanoparticles in medicine: therapeutic applications and developments. *Clin. Pharmacol. Ther.* 83(5), 761–769 (2008).
- 10 Zhang Z, Cao W, Jin H *et al.*: Biomimetic nanocarrier for direct cytosolic drug delivery. *Angew. Chem. Int. Ed. Engl.* 48(48), 9171–9175 (2009).
- **The first paper on cytosolic payload delivery using apolipoprotein A-I mimetic peptide-based nanoparticle.**
- 11 Navab M, Hama S, Hough G, Fogelman AM: Oral synthetic phospholipid (DMPC) raises high-density lipoprotein cholesterol levels, improves high-density lipoprotein function, and markedly reduces atherosclerosis in apolipoprotein E-null mice. *Circulation* 108(14), 1735–1739 (2003).
- 12 Bloedon LT, Dunbar R, Duffy D *et al.*: Safety, pharmacokinetics, and pharmacodynamics of oral apoA-I mimetic peptide D-4F in high-risk cardiovascular patients. *J. Lipid Res.* 49(6), 1344–1352 (2008).
- 13 Cormode DP, Briley-Saebo KC, Mulder WJ *et al.*: An ApoA-I mimetic peptide high-density-lipoprotein-based MRI contrast agent for atherosclerotic plaque composition detection. *Small* 4(9), 1437–1444 (2008).
- 14 Pluen A, Boucher Y, Ramanujan S *et al.*: Role of tumor–host interactions in interstitial diffusion of macromolecules: cranial vs. subcutaneous tumors. *Proc. Natl Acad. Sci. USA* 98(8), 4628–4633 (2001).
- **Important study on the correlation of nanoparticle sizes and solid tumor penetration.**
- 15 Mooberry LK, Nair M, Paranjape S, McConathy WJ, Lacko AG: Receptor mediated uptake of paclitaxel from a synthetic high density lipoprotein nanocarrier. *J. Drug Target* 18(1), 53–58 (2010).
- 16 Cao W, Ng KK, Corbin I *et al.*: Synthesis and evaluation of a stable bacteriochlorophyll-analog and its incorporation into high-density lipoprotein nanoparticles for tumor imaging. *Bioconjug. Chem.* 20(11), 2023–2031 (2009).
- 17 Cao WM, Murao K, Imachi H *et al.*: A mutant high-density lipoprotein receptor inhibits proliferation of human breast cancer cells. *Cancer Res.* 64(4), 1515–1521 (2004).
- 18 Acton S, Rigotti A, Landschulz KT, Xu S, Hobbs HH, Krieger M: Identification of scavenger receptor SR-BI as a high density lipoprotein receptor. *Science* 271(5248), 518–520 (1996).
- **Discovery of scavenger receptor class B type 1 as a receptor for high-density lipoprotein.**
- 19 Rodriguez WV, Thuahnai ST, Temel RE, Lund-Katz S, Phillips MC, Williams DL: Mechanism of scavenger receptor class B type I-mediated selective uptake of cholesteryl esters from high density lipoprotein to adrenal cells. *J. Biol. Chem.* 274(29), 20344–20350 (1999).
- 20 Stevens PJ, Sekido M, Lee RJ: A folate receptor-targeted lipid nanoparticle formulation for a lipophilic paclitaxel prodrug. *Pharm. Res.* 21(12), 2153–2157 (2004).
- 21 Lundberg BB, Risovic V, Ramaswamy M, Wasan KM: A lipophilic paclitaxel derivative incorporated in a lipid emulsion for parenteral administration. *J. Control Release* 86(1), 93–100 (2003).
- 22 Johnstone RW, Ruefli AA, Lowe SW: Apoptosis: a link between cancer genetics and chemotherapy. *Cell* 108(2), 153–164 (2002).
- 23 Corbin IR, Chen J, Cao W, Li H, Lund-Katz S, Zheng G: Enhanced cancer-targeted delivery using engineered high-density lipoprotein-based nanocarriers. *J. Biomed. Nanotech.* 3, 367–376 (2007).
- 24 Mosmann T: Rapid colorimetric assay for cellular growth and survival: application to proliferation and cytotoxicity assay. *J. Immunol. Methods* 65, 55–63 (1983).
- 25 Sanhai WR, Sakamoto JH, Canady R, Ferrari M: Seven challenges for nanomedicine. *Nat. Nanotechnol.* 3(5), 242–244 (2008).
- 26 Panyam J, Labhasetwar V: Targeting intracellular targets. *Curr. Drug Deliv.* 1(3), 235–247 (2004).
- 27 Lacko AG, Nair M, Paranjape S, Mooberry L, McConathy WJ: Trojan horse meets magic bullet to spawn a novel, highly effective drug delivery model. *Chemotherapy* 52(4), 171–173 (2006).
- 28 McConathy WJ, Nair MP, Paranjape S, Mooberry L, Lacko AG: Evaluation of synthetic/reconstituted high-density lipoproteins as delivery vehicles for paclitaxel. *Anticancer Drugs* 19(2), 183–188 (2008).
- 29 Marupudi NI, Han JE, Li KW, Renard VM, Tyler BM, Brem H: Paclitaxel: a review of adverse toxicities and novel drug delivery strategies. *Expert Opin. Drug Saf.* 6(5), 609–621 (2007).
- 30 Zhang Z, Chen J, Ding L, Jin H, Lovell JF, Corbin IR *et al.*: HDL-mimicking peptide-lipid nanoparticles with improved tumor targeting. *Small* 6(3), 430–437 (2010).